Journal of Adhesion Science and Technology

ISSN: 0169-4243 (Print) 1568-5616 (Online) Journal homepage: https://www.tandfonline.com/loi/tast20

Drainage of liquid from a small circular hole in a vertical wall

C. W. Extrand

To cite this article: C. W. Extrand (2018) Drainage of liquid from a small circular hole in a vertical wall, Journal of Adhesion Science and Technology, 32:10, 1142-1149, DOI: 10.1080/01694243.2017.1400802

To link to this article: https://doi.org/10.1080/01694243.2017.1400802

Published online: 14 Nov 2017.

JOURNAL OF ADHESION SCIENCE AND TECHNOLOGY, 2018
VOL. 32, NO. 10, 1142–1149
https://doi.org/10.1080/01694243.2017.1400802

Taylor & Francis
Taylor & Francis Group

Drainage of liquid from a small circular hole in a vertical wall

C. W. Extrand

CPC, Minnesota, MN, USA

ABSTRACT

In this work, the initiation and cessation of flow from a hole in a vertical wall was examined. Water, ethylene glycol or isopropyl alcohol was slowly added to polypropylene (PP) or fluorinated ethylene propylene (FEP) containers with a single circular hole in their side wall. If the hole was sufficiently small, liquid rose past the hole. No liquid flowed through the hole until a critical height was reached. Flow generally ceased before the level of the liquid reached the bottom of the hole. The onset and cessation of flow was successfully modeled as a balance between the hydrostatic pressure in the bulk liquid and the Laplace pressure of the air-liquid interface bulging from the hole.

ARTICLE HISTORY
Received 30 August 2017
Revised 2 October 2017
Accepted 30 October 2017

KEYWORDS
Drainage; wetting; contact angle; surface tension; Laplace pressure

Introduction

The penetration of liquids into porous materials, such as powders and membranes, often is modeled by assuming their pores can be approximated as simple cylindrical holes [1,2]. To flow into or through these materials, a so-called Laplace pressure that arises from the surface tension and curvature of the liquid interface often must be overcome. Discussions of the basic equations for Laplace pressure can be found in textbooks [3–5] and in the scientific literature [6–8]. For example, Padday and colleagues have theoretically examined the shape of pendant and sessile drops attached to various horizontal substrates [7,8].

Somewhat surprisingly, there has been almost no examination of the liquid in contact with a single hole in a vertical substrate. A simple model and experiments are described herein. While certain aspects are intuitive, there were several unexpected findings, such as the role of finite receding contact angles in stopping flow.

Theory

Consider the vertical wall of the container depicted in Figure 1. The top of the container is open and thus exposed to atmospheric pressure. The wall has a round hole of diameter D. As liquid is added to the container and its height rises, the liquid eventually reaches the hole. If the hole is relatively large, then liquid will flow through it. However, if the hole is sufficiently

CONTACT C. W. Extrand chuck.extrand@cpcworldwide.com, chuck.extrand@colder.com

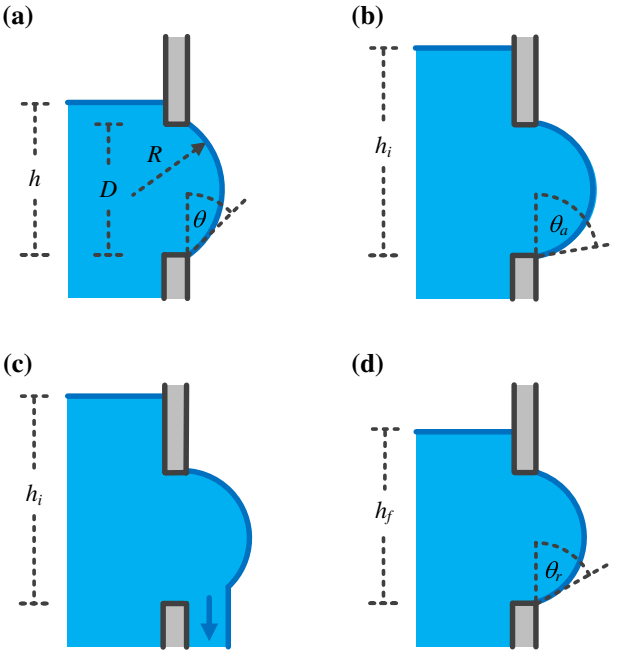

Figure 1. A side, cross-sectional depiction of a fluid handling component with a small circular hole of diameter (D) in one of its vertical walls. (a) Liquid with a surface tension and density of γ and ρ rises vertically past the hole to a height of h without flowing through it. (b) The liquid reaches a critical height of h_i, where $\theta \geq \theta_a$ and (c) flow through the hole begins. (d) As the hole drains, the height of the liquid eventually falls to a critical height of h_f where $\theta \leq \theta_r$ and flow ceases.

small and the wall is sufficiently lyophobic, capillary forces may prevent flow, Figure 1. Here, the air-liquid interface moves through the hole and is pinned at its outer edge. As the height of the liquid continues to rise and hydrostatic pressure increases, the interface, as a result of its motion, bulges outward from the vertical wall. The radius of curvature (R) of the protruding liquid interface along with its surface tension (γ) creates a so-called Laplace pressure (Δp_L), which is directed inward against the bulk liquid. For a circular hole [9],

$$\Delta p_L = \frac{2\gamma}{R}. \tag{1}$$

As the liquid rises, the hydrostatic pressure increases. In response, the radius of curvature of the bulging liquid decreases, while the contact angle (θ) between the liquid and the exterior surface of the vertical wall increases. If it is assumed that the shape of the liquid bulging from the hole can be approximated as a section of sphere, then its radius of curvature (R) and the hole diameter (D) are related through the sine function,

$$\sin\theta = \frac{D/2}{R}. \tag{2}$$

The hydrostatic pressure (Δp_h) in the bulk liquid depends upon the height of the liquid above the bottom of the hole (h), the liquid density (ρ) and the acceleration due to gravity ($g = 9.81\ \mathrm{m/s^2}$),

$$\Delta p_h = \rho g h. \tag{3}$$

If no liquid flows through the hole, then the Laplace and hydrostatic pressures are equal,

$$\Delta p_L = \Delta p_h. \tag{4}$$

Substituting Equations (1)–(3) into (4) produces general equations for estimating the minimum height of liquid to initiate flow. If the wall is relatively lyophilic ($\theta_a < 90°$), then rising liquid will trigger flow through the hole when the liquid bulges sufficiently that $\theta = \theta_a$. Here, the height of liquid required to initiate flow (h_i) is

$$h_i = \frac{4\gamma}{\rho g D} \sin \theta_a. \tag{5}$$

For lyophobic walls ($\theta_a \geq 90°$), flow begins before the liquid attains an advancing contact angle on the vertical wall. The maximum Laplace pressure occurs where $\theta = 90°$ [4,7,8] and consequently,

$$h_i = \frac{4\gamma}{\rho g D}. \tag{6}$$

As liquid drains, the hydrostatic pressure in the hole diminishes. If the receding contact angle (θ_r) of the external wall is > 0, then drainage stops before $h = 0$. Ignoring any kinetic contributions, the final height of the liquid (h_f) where flow ceases can similarly be estimated by balancing Laplace and hydrostatic pressures. For surfaces where $\theta_r < 90°$,

$$h_f = \frac{4\gamma}{\rho g D} \sin \theta_r. \tag{7}$$

Otherwise, if $\theta_r \geq 90°$,

$$h_f = \frac{4\gamma}{\rho g D}. \tag{8}$$

Experimental details

Liquids

The liquids used were isopropyl alcohol (IPA, Pharmco-Aaper, 99% Reagent ACS grade), ethylene glycol (EG, Fisher Scientific, BP230-1) and de-ionized water (W). Values of their surface tension (γ) and density (ρ), listed in Table 1, were taken from the literature [4,10]. The uncertainty γ and ρ was estimated to be ±1 mN/m and ±2 kg/m^3.

Solids

The walls of the fluid handling components were either polypropylene (PP, Rubbermaid LunchBlox Pack Snack Containers, Part # 7P88, 2.33 in long × 2.73 in wide × 2.23 in high,

Table 1. Properties of the liquids.

Liquid	γ (mN/m)	ρ (kg/m^3)
Isopropyl alcohol (IPA)	22	789
Ethylene glycol (EG)	47	1110
Water (W)	72	998

0.5 cup or ~120 ml) or fluorinated ethylene propylene (FEP, McMaster Carr, 3/32 × 6 ×6 inch sheet, Part # 85375K213), which is a polytetrafluoroethylene (PTFE) copolymer.

For PP, a single round hole of diameter D was machined in the side wall of the Rubbermaid containers using an end mill (1/16–1/4 inch diameter) installed in a Bridgeport mill. For FEP, small square coupons (roughly 2 × 2 cm^2) were cut with a jigsaw and a round hole was milled in the center of each coupon. After measuring wettability, the FEP coupon was adhered to the side wall of a PP container over a ¼ inch hole using a silicone adhesive (GE Premium Silicone Glue, Silicone II Clear). The uncertainty in D was approximately ±0.05 mm.

Contact angles

Advancing and receding contact angles on the solid surfaces were determined as follows. For PP, each container was placed on the stage of an optical microscope (Keyence VHX-5000) with its hole facing up. A liquid drop with a volume (V_a) of 10 μL was deposited on the PP with a syringe (Hamilton, Model 1701 N) and allowed to spread. Resident software in the microscope was used to measure the base diameter ($2a_a$) of the resulting 'advancing' sessile drop. Next, liquid was withdrawn until the contact line receded, the remaining volume of liquid and the diameter of the resulting 'receding' sessile drop (V_r and $2a_r$) were noted. Values of V_r ranged from 1 to 4 μL. The volume of the liquid used to produce sessile drops on PP, 10 μL or less, was sufficiently small that gravity did not distort their shape, allowing for indirect estimates of contact angles from drop dimension and volume [11],

$$\theta_i = 2 \cdot \mathrm{ArcTan}\left\{\frac{\left[\frac{48V_i}{\pi(2a_i)^3} + \left(4 + \left(\frac{48V_i}{\pi(2a_i)^3}\right)^2\right)^{1/2}\right]^{2/3} - 2^{2/3}}{2^{1/3}\left[\frac{48V_i}{\pi(2a_i)^3} + \left(4 + \left(\frac{48V_i}{\pi(2a_i)^3}\right)^2\right)^{1/2}\right]^{1/3}}\right\}, \tag{9}$$

where $i = a$ for advancing angles and $i = r$ for receding ones.

For FEP, contact angles were measured using a digital goniometer (Kyowa DMs-401) before attaching the FEP coupons to the PP containers. The FEP coupons were placed on stage of the goniometer, 10 μL water drop was deposited on FEP, and then one second later, its height (H) and base dimeter ($2a$) were automatically recorded. These dimensions were used to estimate advancing contact angles [12–14],

$$\theta_a = 2 \cdot \mathrm{ArcTan}\frac{2H}{2a}. \tag{10}$$

To measure receding angles on FEP, water was withdrawn from 10 μL sessile drops until the contact line retracted. With the needle of the syringe still contacting the drop, an image was captured. Base and tangent lines were constructed on the sessile drop image and θ_r was measured directly.

Advancing and receding contact angles (θ_a and θ_r) of the various liquid-solid combinations are listed in Table 2. Values of θ_a and θ_r ranged from 107° for water on FEP to 5° for IPA on FEP. Standard deviation and uncertainty in the contact angle measurements was generally ± 2°, but greater (~ ±5°) for near-zero values [11].

Table 2. Advancing and receding contact angles (θ_a and θ_r) of the various liquids on the solids.

Solid	Liquid	θ_a (°)	θ_r (°)
PP	IPA	15	5
	EG	68	54
	W	90	69
FEP	W	107	93

Drainage experiments

Containers were placed on a slight incline to vertically orient the wall with the hole. Liquid was gently poured from a 10 mL graduated cylinder into the container. At the instant that liquid flowed out of the circular hole, an image was captured with an Apple iPhone 5s. When flow through the hole ceased, another photo was taken. Values of h_i and h_f were measured from the subsequent images. Five replicates were performed for each liquid-solid-hole combination. The standard deviation in h_i and h_f values was 0.1 to 0.8 mm. Error propagation techniques involving partial derivatives [15] (logarithmic differential method) suggested that the uncertainty in h_i and h_f could have been as high as ± 0.4 to 0.7 mm. All measurements were made at (22 ± 1) °C.

Results and discussion

Figure 2 shows plots of the critical liquid heights to initiate and terminate flow (h_i and h_f) through a small circular hole of diameter D. The points are experimental data. The error bars represent standard deviation in the measurements. The height to initiate flow is greatest for small holes and declined precipitously as D increased. For water in PP, h_i values ranged from 18.8 to 4.7 mm. For holes of equal D, liquid-solid combinations with larger values of γ and θ_a demonstrated greater resistance to flow.

Even though FEP is more hydrophobic than PP, values of h_i for water were nearly identical for these two solids. Water began to flow through the hole in FEP where $\theta = 90°$. In contrast, the impediment to flow of IPA was minimal, due to a combination of low surface tension and contact angles. The height at which flow ceased (h_f) also decreased with D. Note that if θ_r was effectively zero, then then drainage continued until the liquid level fell all the way to the bottom of the hole; for IPA, $\theta_r \sim 5°$ and $h_f \sim 0$. While the outer surface surrounding the hole was important in determining the onset and cessation of flow, the inner surface was not. Machining created burrs on the inner surface of the PP container. In some cases, the burrs were cut away. However, the presence or absence of the burrs had no effect.

The curves in Figure 2 are theoretical estimates from Equations (6)–(9). The black, solid curves are for water (W), the green, short-dash curves are for ethylene glycol (EG) and the blue, long-dash curves are for isopropyl alcohol (IPA). Agreement between measured and predicted h_i values were excellent. On the other hand, predicted values of h_f were reasonable for larger diameter holes, but underestimated h_f for smaller holes. For example, water ceased to flow from a PP container with D = 1.7 mm at h_f = 13.5 mm. In this case, Equation (8) over predicted h_f to be 17.3 mm.

It was supposed that smaller holes led to higher hydrostatic pressures and greater flow velocities, which in turn reduced h_f. Equation (8) was modified to include the influence of inertia,

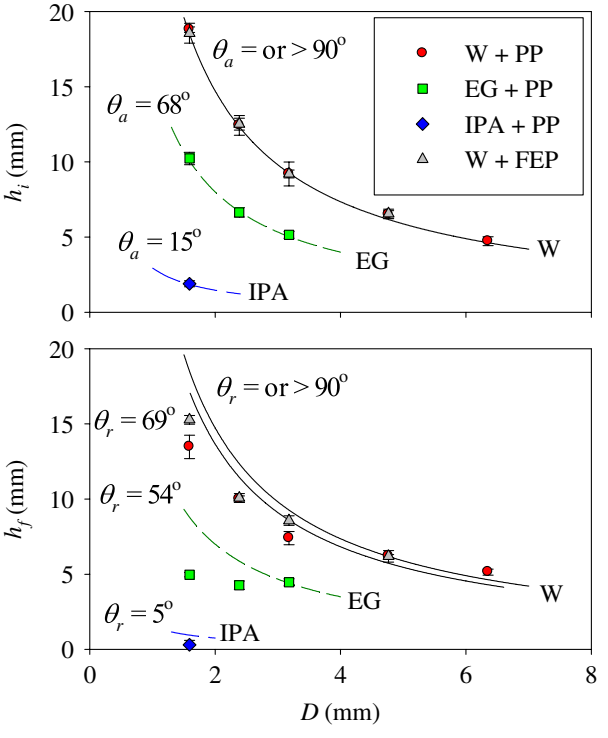

Figure 2. Plots of the critical liquid heights to initiate and terminate flow (h_i and h_f) through a small circular hole of diameter D. The points are experimental data. The error bars represent standard deviation in the measurements. The curves are theoretical estimates from Equations (6)–(9). The black, solid curves are for water (W), the green, short-dash curves are for ethylene glycol (EG) and the blue, long-dash curves are for isopropyl alcohol (IPA).

$$h_f = \frac{1}{g}\left(\frac{4\gamma}{\rho D}\sin\theta_r - \frac{1}{2}v^2\right), \tag{11}$$

where v is the velocity of liquid flowing through the hole. For the previous example of the PP container with $D = 1.7$ mm, where v was experimentally measured to be ~0.3 m/s, Equation (12) lends a more accurate prediction, $h_f = 12.7$ mm. (Details regarding the derivation of Equation (12) are given in the Appendix 1.)

It is noteworthy that the onset of drainage can be considered as an adhesion phenomenon, where two distinct modes exist. If $\theta_a < 90°$, then drainage is initiated by an adhesive failure between the liquid and solid along the contact line at the bottom of the bulge. Conversely, if the $\theta_a \geq 90°$, then a cohesive failure in the liquid interface instigates flow.

Work here has focused on millimeter-sized holes where h_i and $h_f > D$. In principle, the model should also be applicable for much smaller, micron size holes. It also probably would be valid for a circular hole in horizontal wall. An interesting topic for future study could be the case where $h_i < D$. This is likely to be more challenging due to the complex, non–axisymmetric shape of the liquid interface in a partially filled hole.

Conclusions

Small holes in the vertical walls of liquid handling components can prevent flow. Curvature and surface tension of the liquid counteract flow driven by hydrostatic pressure. Resistance to flow increases as the hole gets smaller, as surface tension of the liquid increases or as liquid density decreases. Wettability also plays an important role in the onset and cessation of flow; larger advancing contact angles increase resistance to flow.

Acknowledgements

Thanks to M. Acevedo, D. Ball, D. Burdge, L. Castillo, J. Doyon, L. Hoelscher, K. Long, K. Sekeroglu, K. Switalla, K. Vangsgard, J. Wittmayer and G. Zeien for their help and support.

Disclosure statement

No potential conflict of interest was reported by the author.

References

[1] Lucas R. Ueber das Zeitgesetz des Kapillaren Aufstiegs von Flussigkeiten. Kolloid Z. 1918;23(1):15.
[2] Washburn EW. Note on a method of determining the distribution of pore sizes in a porous material. Proc Natl Acad Sci USA. 1921;7(4):115–116.
[3] Wu S. Polymer interface and adhesion. New York (NY): Marcel Dekker; 1982.
[4] Adamson AW. Physical chemistry of surfaces. 5th ed. New York (NY): Wiley; 1990.
[5] Hiemenz PC, Rajagopalan R. Principles of colloid and surface science. 3rd ed. New York (NY): CRC Press; 1997.
[6] Bashforth F, Adams JC. An attempt to test the theories of capillary action by comparing the theoretical and measured forms of drops of fluid. Cambridge: University Press; 1883.
[7] Padday JF, Pitt A. Axisymmetric meniscus profiles. J. Colloid Interface Sci. 1972;38(2):323–334.
[8] Padday JF, Pitt AR. The stability of axisymmetric menisci. Proc R Soc Lond A. 1973;275(1253):489–528.
[9] Laplace, PS. Mécanique Celeste. Paris: Courier; 1805; Vol. t. 4, Supplément au X^{e} Livre.
[10] Weast RC. Handbook of chemistry and physics. 73rd ed. Boca Raton (FL): CRC; 1992.
[11] Extrand CW, Moon SI. When sessile drops are no longer small: transitions from spherical to fully flattened. Langmuir 2010;26(14):11815–11822.
[12] Mack GL. The determination of contact angles from measurements of the dimensions of small bubbles and drops. I. The spheroidal segment method for acute angles. J Phys Chem. 1936;40(2):159–167.
[13] Mack GL, Lee DA. The determination of contact angles from measurements of the dimensions of small bubbles and drops. II. The sessile drop method for obtuse angles. J Phys Chem. 1936;40(2):169–176.
[14] Bartell FE, Zuidema HH. Wetting characteristics of solids of low surface tension such as talc, waxes and resins. J Am Chem Soc. 1936;58(8):1449–1454.
[15] Taylor JR. An introduction to error analysis. 2nd ed. Sausalito (CA): University Science Books; 1997.

Appendix 1

The onset of flow and cessation of flow at low rates is explained above in terms of a balance between hydrostatic and Laplace pressures. For higher flow rates, it is reckoned that inertia becomes important. Thus, for higher flow rates, a term for Bernoulli pressure (Δp_v) can be added to Equation (4),

$$\Delta p_L = \Delta p_h + \Delta p_v, \tag{12}$$

where

$$\Delta p_v = \tfrac{1}{2}\rho v^2. \tag{13}$$

Combining Equations (1)–(3) with Equations (13) and (14) gives an expression for estimating the height at which flow stops (h_f),

$$h_f = \frac{1}{g}\left(\frac{4\gamma}{\rho D}\sin\theta_r - \frac{1}{2}v^2\right). \tag{14}$$